NANO LETTERS

pubs.acs.org/NanoLett Letter

Chiral Phonon Diode Effect in Chiral Crystals

Hao Chen, Weikang Wu, Jiaojiao Zhu, Zhengning Yang, Weikang Gong, Weibo Gao,* Shengyuan A. Yang,* and Lifa Zhang*

Cite This: *Nano Lett.* 2022, 22, 1688−1693 Read Online

ACCESS | Metrics & More | Article Recommendations | Supporting Information

ABSTRACT: The diode effect means that carriers can only flow in one direction but not the other. While diode effects for electron charge, spin, or photon have been widely discussed, it remains a question whether a chiral phonon diode can be realized, which utilizes the chiral degree of freedom of lattice vibrations. In this work, we reveal an intrinsic connection between the chiralities of a crystal structure and its phonon excitations, which naturally leads to the chiral phonon diode effect in chiral crystals. At a certain frequency, phonons with a definite chirality can propagate only in one direction but not the opposite. We demonstrate the idea in concrete materials including bulk Te and α-quartz (SiO_2). Our work discovers the fundamental physics of chirality coupling between different levels of a system, and the predicted effect will provide a new route to control phonon transport and design information devices.

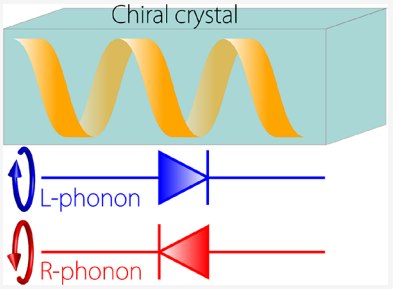

KEYWORDS: *chiral crystals, chiral phonon diode effect, chirality filtering, chirality-orbit coupling, pseudoangular momentum, first-principles calculations*

The concept of chirality plays a significant role in multiple branches of sciences, such as physics, chemistry, and biology.[1−3] An object or a structure is chiral if it is distinguished from its mirror image. In other words, all possible mirror (inversion) symmetries of the structure must be broken. Such chiral structures are ubiquitous, ranging from microscopic molecules to astronomical objects, and they have found wide applications, for example, in enantioselective catalysis,[4] chiral drug design,[5] chiral-induced spin selectivity,[6−8] and so forth.

Chirality also applies to the description of collective excitations of a system. A notable example from recent research is the chiral phonon,[9] that is, the collective oscillation modes of a crystal lattice with a definite handedness. It has been shown that chiral phonons can couple with circularly polarized light and valley electrons and result in chiral selective optical transitions.[10−14] They therefore serve as promising information carriers. It was also proposed that chiral phonons can make important contributions to the thermal conductivity,[15] phononic Hall effect,[16,17] orbital magnetization,[18−20] and anomalous thermal expansion.[21]

Now, a natural question is the following: Is there any interplay between chiral phonons and the chirality of the underlying lattice? This important question has remained unexplored. The research so far mainly focused on achiral structures. Intuitively, for an achiral system each chiral phonon mode must have a chiral partner connected by a mirror operation, which poses difficulty to single out one chirality.

In this work, we address the above question by exploring chiral phonons in chiral crystals. We reveal a strong coupling between the chiralities of the two, which naturally leads to a chiral phonon diode effect, that is, the input chirality information can only pass the system via chiral phonons in one way but not the other, as specified by the system chirality. Specifically, we show that a propagating chiral phonon mode in a chiral crystal has its propagation direction determined by the lattice chirality. At certain fixed frequency, phonons with opposite chiralities propagate in opposite directions. The phonon chirality or the propagation direction is switched when the crystal is changed to its enantiomorph. These results are confirmed via explicit calculations on a helix-chain model and demonstrated in bulk Te as well as a common and important 3D material, α-quartz. Our work discovers a fundamental connection between the chiralities of a structure and its excitations, which opens a new direction for phononic research. The predicted chirality diode effect may enable new routes for controlling phonon transport and for designing information devices.

Helix-Chain Model. To capture the essential physics, we first consider the simplest chiral lattice model, a 1D helix chain. As illustrated in Figure 1, the simplest helix has three sites in a unit cell, and its handedness can be readily determined from its spiral pattern: Figure 1a,b shows right- and left-handed chains, respectively. Clearly, the helix structure breaks all possible

Received: December 6, 2021
Revised: February 7, 2022
Published: February 11, 2022

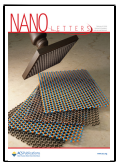

https://doi.org/10.1021/acs.nanolett.1c04705
Nano Lett. 2022, 22, 1688−1693

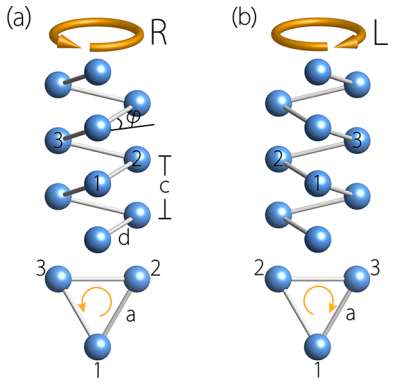

Figure 1. (a) Right-handed and (b) left-handed 1D helix chain model. The bottom panel shows the top view. The structural parameters are marked in (a).

mirrors, yet for a regular helix, it preserves a three-fold screw axis $S_{3z} = \left\{C_{3z}\middle|00\frac{1}{3}\right\}$ along the chain (z-direction). In the ground state (that is, without oscillation), the chiral structure can be specified by a few parameters, as indicated in Figure 1a. Here, the top view is an equilateral triangle with side length a, d is the bond length between two neighboring sites, $\varphi = \arccos(a/d)$ is the tilt angle of a bond from the $x-y$ plane, and the helix period $c = 3a \tan\varphi$.

The harmonic oscillations of the lattice is described by the standard Hamiltonian

$$\mathcal{H} = \frac{1}{2}\mathbf{p}^{\mathrm{T}}\mathbf{p} + \frac{1}{2}\mathbf{u}^{\mathrm{T}}\mathbf{K}\mathbf{u} \tag{1}$$

where $\mathbf{u}$ is a column vector of displacements from the equilibrium positions, multiplied by the square root of mass (the mass is taken to be the same for every site here); $\mathbf{p}$ is the conjugate momentum vector, and $\mathbf{K}$ is the force constant matrix. For simplicity, we retain only the nearest-neighbor coupling. These parameters, along with the structural parameters such as φ, specify the matrix $\mathbf{K}$. The phonon spectrum $\omega_{k,\sigma}$ and the phonon eigenmodes $\epsilon_{k,\sigma}$ are then solved from the equation

$$D(k)\epsilon_{k,\sigma} = \omega_{k,\sigma}^2\epsilon_{k,\sigma} \tag{2}$$

where k is the 1D wave vector along the chain, the dynamic matrix $\mathbf{D}(k)$ is the spatial Fourier transform of $\mathbf{K}$, and the index σ labels the phonon branch.

The calculated phonon spectra of right- and left-handed helices are plotted in Figure 2a,b, which consist of three acoustic branches and six optical branches, corresponding to the three sites in a unit cell. Particularly, to investigate the chirality of phonon modes, we use the color map in Figure 2a,b to indicate the value of phonon circular polarization along the chain, which is defined by[9]

$$s_{k,\sigma} = \epsilon_{k,\sigma}^{\dagger}\hat{S}_z\epsilon_{k,\sigma} \tag{3}$$

where $\hat{S}_z = \sum_{\alpha=1}^{3}(|R_\alpha\rangle\langle R_\alpha| - |L_\alpha\rangle\langle L_\alpha|)$ is the circular polarization operator, $|R_\alpha\rangle$ ($|L_\alpha\rangle$) is the right (left) circularly polarized oscillation basis at site α (for circular motion in the $x-y$ plane). It was shown in ref 9 that $\hbar s_{k,\sigma}$ gives the angular momentum of the phonon mode $\epsilon_{k,\sigma}$ along the chain. The sign of $s_{k,\sigma}$ indicates the chirality, namely, the phonon mode is right (left) handed if $s_{k,\sigma} > 0$ (< 0).

From the results in Figure 2a, first of all, one can clearly see that the phonon modes are chiral. The inset shows the vibration pattern of the mode P indicated by the black dot in Figure 2a. One observes that from top view, all three sites make clockwise rotations, confirming its left-handed chirality. This is in contrast with an achiral chain. For example, if the chain preserves a mirror (denoted by M) that contains the chain axis, then each mode $\epsilon_{k,\sigma}$ would be degenerate with a mirror partner $M\epsilon_{k,\sigma}$, such that there is no net circular polarization nor chirality of the phonons.

Second, the chiral phonons can generally propagate along the chain. The propagation direction is determined by the sign of the slope of the dispersion. From the result, one observes a chirality-orbit coupling, that is, the chirality of a phonon is coupled with its propagation, analogous to the spin−orbit coupling. Importantly, there exist frequency windows in which the chirality is completely locked with the propagation direction. For example, consider the frequency at mode P in Figure 2a. At this frequency, there are only two phonon modes. The one that propagates in the z-direction is left-handed, whereas that propagates in the $-z$ direction is right-handed, as dictated by the time reversal symmetry. Thus, the helix chain acts as a chiral phonon diode when operated at this frequency: a phonon with a definite chirality can only pass the system in

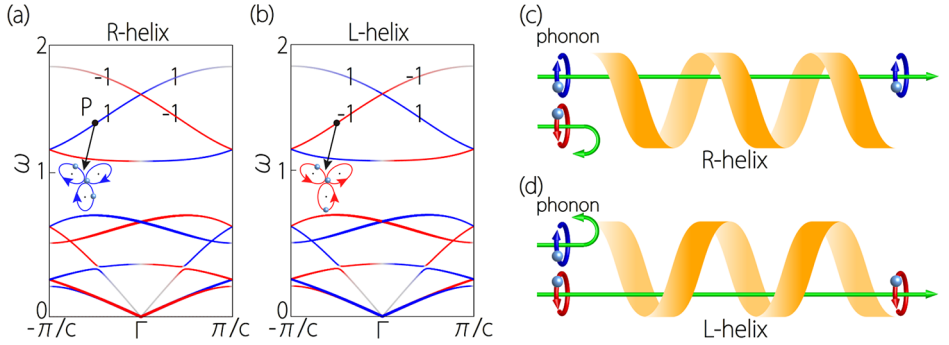

Figure 2. Calculated phonon spectra for (a) right-handed helix and (b) left-handed helix. They show the same dispersion but opposite chirality distribution. The red and blue colors represent the right and left circularly polarized phonon modes, respectively. The PAM for the top two phonon branches are marked. The inset shows the top view of the phonon vibration pattern for the mode marked by the black dot. The calculation details and model parameters are presented in the Supporting Information. (c,d) Schematic diagram of the chirality filtering. (c) At the frequency around P in (a), only left-handed phonons are allowed to pass the helix from left to right. (d) The situation reverses when the chirality of the helix is switched.

https://doi.org/10.1021/acs.nanolett.1c04705
Nano Lett. 2022, 22, 1688−1693

one way but not the other. In addition, if we only consider the transport from left to right, the helix can also be viewed as a chirality filter: as shown in Figure 2c, the system allows the left-handed phonon to pass through, but not the right-handed one; and the situation is reversed for propagation in the opposite direction.

Third, as mentioned, the helix chain here preserves a three-fold screw rotational symmetry S_{3z}. It allows the definition of a pseudoangular momentum (PAM)[9] $l_{k,\sigma}$ for phonons, which just corresponds to the eigenvalues of a phonon mode under three-fold rotation (the fractional translation part can be disregarded as it does not affect any selection rules to be discussed later). Explicitly, we have

$$\mathcal{R}_z[(2\pi/3)]\epsilon_{k,\sigma} = e^{-i(2\pi/3)l_{k,\sigma}}\epsilon_{k,\sigma} \quad (4)$$

where $\mathcal{R}_z$ is the rotation operator acting on the eigenmode and is defined to connect the three sites, and the PAM defined in this way is an integer $\in \{0, \pm 1\}$. For example, the PAM for the top two phonon branches is labeled in Figure 2a. One observes that PAM is also coupled with the chirality and the propagation direction. Phonons with PAM + 1 travel in the + z direction, whereas those with −1 go the opposite way.

Finally, it is crucial and evident that the phonon chirality (and the PAM) is tied with the chirality of the lattice. The results above are for the right-handed helix. For a left-handed helix, the phonon chirality would be flipped, as in Figure 2b. The system allows the right-handed phonon to pass through from left to right, but not the left-handed one, as shown in Figure 2d. This also justifies that for the achiral structure, which may be regarded as the phase boundary between the right- and the left-handed helices, the phonon chirality as well as the associated effects such as chirality-orbit coupling and chiral phonon diode effect must vanish.

Application to Bulk Te. To demonstrate our proposed physics in concrete materials, we first consider bulk Te, because its structure is directly connected to the model discussed above. As shown in Figure 3a,b, bulk Te can be viewed as an array of 1D Te helix chains which are all of the same chirality. The space group for the right-handed bulk Te chain is $P3_121$ (No. 152), whereas that for the left-handed one is $P3_221$ (No. 154). Both structures preserve a three-fold screw axis, but the screw directions are opposite. In Figure 3d, we plot the phonon spectrum of right-handed bulk Te obtained from first-principles calculations. The calculation details are given in the Supporting Information. We evaluate the phonon circular polarization $s_{k,\sigma}$, which confirms that the phonons here are generally chiral.

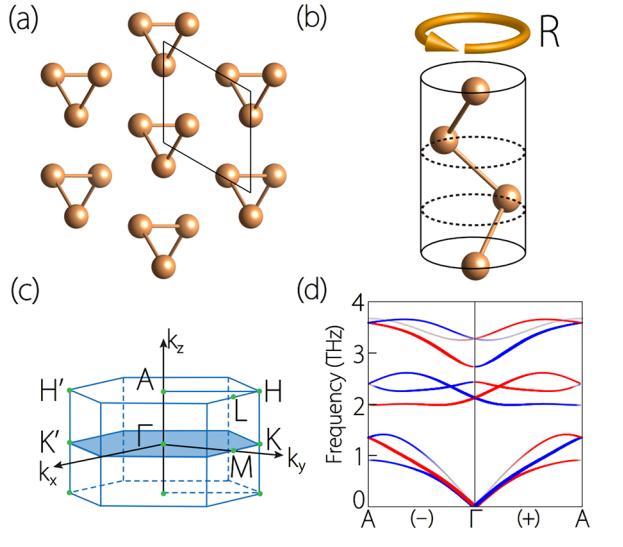

Figure 3. (a) Top view of the right-handed bulk Te. The black box marks the unit cell. (b) Side view of a single Te chain. It shows a right-handed helix structure. (c) Brillouin zone. (d) Phonon spectrum of the right-handed bulk Te. +/− on the path indicates the $k_z > 0/k_z < 0$ part. Red/blue color represents right/left-handed phonons.

We are particularly interested in the phonons on the high-symmetry paths that preserve the screw rotation, because these modes further allow a well-defined PAM. These paths include Γ−A, K−H, and K'−H' in the Brillouin zone (Figure 3c). Note that each path has two sections: the section with $k_z > 0$ and the one with $k_z < 0$. To distinguish the two, we shall label the former/latter one by adding a plus/minus sign. For instance, the two sections along the k_z axis will be labeled as Γ−$A(+)$ and Γ−$A(-)$, respectively. At a certain frequency, the phonon chirality is coupled with the propagation direction. This confirms the features of chirality-orbit coupling and chirality diode/filtering which we learned from the helix model. The PAM for each phonon branch is presented in the Supporting Information.

It is important to note that the emergence of chiral phonons on the Γ−A path is a manifestation of the chirality of the system. For 3D achiral crystals, such as WN_2 discussed in ref 14, phonon modes on this path do not have net chirality, since each left-handed mode must be accompanied by a right-handed partner. In addition, the property of chirality diode/filtering is generally not expected for an achiral crystal: a branch can have the same chirality on K−$H(+)$ and K−$H(-)$, as shown in ref 14.

The results above are for the right-handed Te. Evidently, for the left-handed crystal the phonon spectrum would look the same, but the phonon chirality and PAM would be flipped.

Application to α-Quartz. It appears natural to have the proposed effects manifest in bulk Te, as its structure exhibits a quasi-1D character consisting of helix chains. To show that the physics is general, below we extend the discussion to another concrete 3D material, α-quartz, which is a stable crystal polymorph of SiO_2 that is most commonly found in nature.[22] α-quartz has important applications in many industrial branches, ranging from construction to electronics. The lattice structure of quartz consists of SiO_4 tetrahedra linked by shared corner oxygens. Importantly, the α-quartz lattice is chiral. It crystallizes in two enantiomorphic space groups, $P3_121$ (No. 152) and $P3_221$ (No. 154),[23,24] depending on the chirality. Figure 4a,b shows the structure of the right-handed α-quartz with space group $P3_121$. One observes that along the c-axis, the SiO_4 tetrahedra spiral upward in a right-handed way, resembling the helix in Figure 1a. However, there is no isolated helix chain. All the tetrahedra are strongly covalently bonded into a 3D network.

In Figure 4c, we show the phonon dispersion of right-handed α-quartz calculated by first-principles calculations. There are a total of twenty-seven phonon branches, corresponding to the nine atoms in the unit cell. We see that the 17th and 18th phonon branches around 16−22 THz are well separated from other branches, which gives an advantage for their excitation and detection. Focusing on these two branches, in Figure 4c we use the color map to show the calculated phonon circular polarization on the high-symmetry

https://doi.org/10.1021/acs.nanolett.1c04705
Nano Lett. 2022, 22, 1688−1693

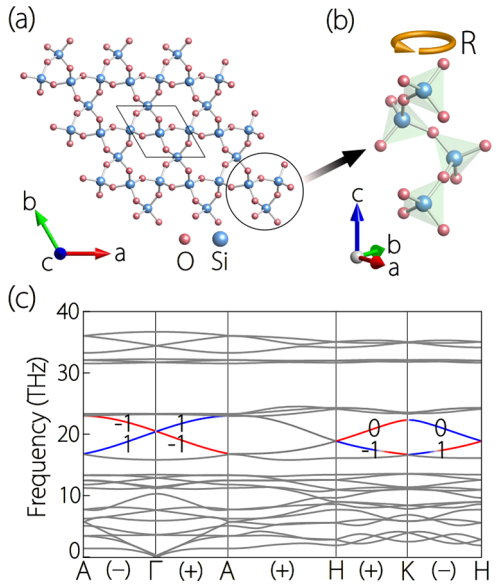

Figure 4. (a) Top view of the right-handed α-quartz (SiO_2): the black box marks the unit cell. (b) Side view of the vertical chain structure marked by the black circle in (a). It shows a right-handed helix structure. (c) Phonon spectrum of the right-handed α-quartz. + /− on the path indicate the $k_z > 0/k_z < 0$ part. For the two phonon branches with energy in the range of 16−22 THz, we marked the phonon chirality and PAM. Red/blue color represents right/left-handed phonons.

paths. Clearly, one observes that these phonons are chiral. For instance, the phonons of the 18th branch on the $\Gamma-A(+)$ are left-handed and propagate in the $+z$ direction, whereas the corresponding ones on $\Gamma-A(-)$ are right-handed and propagate in the $-z$ direction.

In Figure 4c, we have also labeled the phonon PAM for the 17th and 18th branches. One can see that the PAMs for $\Gamma-A(+)$ and $\Gamma-A(-)$ also differ by a minus sign, as dictated by the time reversal symmetry. The PAM determines selection rules for phonon coupling with other particles. For example, a circularly polarized light incident along the z-direction can excite a phonon mode subjected to the PAM conservation: $m = l \bmod 3$, where $m = \pm 1$ for right/left circularly polarized light. This allows a selective coupling between chiral phonons and infrared light.

Discussion. We have discovered an intrinsic connection between the chiralities of a structure and its phonon excitations. We find that chiral structures host chiral phonons on the principal axis through Γ which exhibit chirality-orbit coupling, chiral phonon diode effect, chirality filtering, and net PAM, all distinct from achiral systems, and these properties are reversed when the structural chirality is flipped.

Our proposed chiral phonon diode effect can be detected in experiment. Consider a slab of a chiral crystal, for example, of right-handed α-quartz, with its c-axis along the z-direction. We apply a circularly polarized infrared light with a frequency peaked around 21 THz (that is, the range of the 18th branch in Figure 4c) incident on the bottom of the slab, as shown in Figure 5a. Because of the PAM conservation, a right/left circularly polarized light can resonantly excite phonon modes with PAM +1/−1. Meanwhile, due to the momentum conservation light can only excite phonons on the $\Gamma-A$ paths. (Note that the slab surface breaks the translation symmetry along z, so k_z needs not to be conserved.) Therefore,

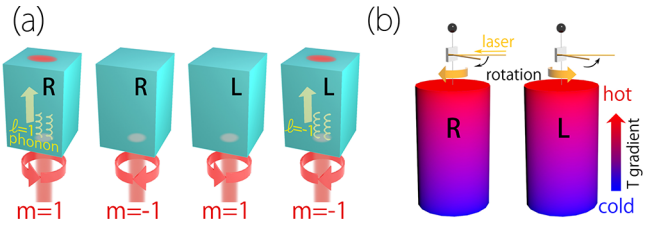

Figure 5. (a) Schematic experimental setup for detecting chiral phonon diode effect. R and L on the sample indicate right-handed and left-handed lattices, respectively. The bottom of the sample is shined with a circularly polarized light. The chirality diode effect manifests as the temperature difference on the top surface depending on the light polarization and the lattice chirality. (b) When a hanged α-quartz sample is applied with a temperature gradient. The chiral phonons will induce a rotation of the sample and the rotation direction depends on the crystal chirality. See the main text for more descriptions.

the incident light with right (left) circular polarization will mostly excite chiral phonons with PAM +1(−1) on the $\Gamma-A$ path. However, due to the chiral phonon diode effect, in this frequency range, only the phonons with PAM + 1 are propagating in the $+z$ direction, that is, can pass through the slab. Since phonons are important for heat conduction (electronic contributions here can be neglected as α-quartz are good insulator with a band gap ~5.8 eV), in experiment, by switching the circular polarization of the incident light, the chiral phonon diode effect can manifest as a temperature difference detected on the top surface of the slab, as illustrated in Figure 5a.

Because of the chirality-orbit coupling, when a temperature gradient along the c-axis is applied across the sample, the nonequilibrium phonon distribution $f_{k,\sigma}$ will generally cause a nonzero net phonon circular polarization $S = \sum_{k,\sigma} s_{k,\sigma} f_{k,\sigma}$ and hence a nonzero phonon angular momentum $\hbar S$.[18,25] This thermally generated phonon angular momentum can be detected by the rotation of a hanged cylinder-shaped sample similar to the Einstein-de Haas effect,[26] as shown in Figure 5(b). From our calculations, the resulting angular velocity for α-quartz is $\omega \sim \frac{\Delta T/(1\ \mathrm{K})}{\hbar r^2/(1\ \mathrm{m})^3} \times 10^{-20}\ \mathrm{s}^{-1}$ (For more calculation details, please see the Supporting Information). Assuming that the radius and the height of the sample are $r = 10\ \mu$m and $h = 100\ \mu$m, and the applied temperature difference between the top and the bottom surfaces $\Delta T = 10$ K, then the resulting ω can reach $\sim 10^{-5}\ \mathrm{s}^{-1}$, which can be detected in experiment. In addition, for ionic crystals, the chiral phonons may also carry a magnetic moment. Then the net phonon angular momentum is accompanied by an induced magnetization, which can be detected by magnetism probes. Again, all these signals are tied with the chirality of the crystal: the signals should switch signs when we change a right-handed sample with a left-handed one.

■ ASSOCIATED CONTENT

Supporting Information

The Supporting Information is available free of charge at https://pubs.acs.org/doi/10.1021/acs.nanolett.1c04705.

The parameters of helix-chain model, first-principles calculations details, opposite total angular momentum effect, electronic band structure of α-quartz and the calculated PAM of chiral Te lattice (PDF)

https://doi.org/10.1021/acs.nanolett.1c04705
Nano Lett. 2022, 22, 1688−1693

AUTHOR INFORMATION

Corresponding Authors

Weibo Gao − *Division of Physics and Applied Physics, School of Physical and Mathematical Sciences, Nanyang Technological University, Singapore 637371, Singapore;* orcid.org/0000-0003-3971-621X; Email: wbgao@ntu.edu.sg

Shengyuan A. Yang − *Research Laboratory for Quantum Materials, Singapore University of Technology and Design, Singapore 487372, Singapore*; Email: shengyuan_yang@sutd.edu.sg

Lifa Zhang − *NNU-SULI Thermal Energy Research Center and Center for Quantum Transport and Thermal Energy Science (CQTES), School of Physics and Technology, Nanjing Normal University, Nanjing 210023, China;* orcid.org/0000-0001-6108-1404; Email: phyzlf@njnu.edu.cn

Authors

Hao Chen − *NNU-SULI Thermal Energy Research Center and Center for Quantum Transport and Thermal Energy Science (CQTES), School of Physics and Technology, Nanjing Normal University, Nanjing 210023, China; Division of Physics and Applied Physics, School of Physical and Mathematical Sciences, Nanyang Technological University, Singapore 637371, Singapore;* orcid.org/0000-0003-3296-670X

Weikang Wu − *Division of Physics and Applied Physics, School of Physical and Mathematical Sciences, Nanyang Technological University, Singapore 637371, Singapore; Research Laboratory for Quantum Materials, Singapore University of Technology and Design, Singapore 487372, Singapore*

Jiaojiao Zhu − *Research Laboratory for Quantum Materials, Singapore University of Technology and Design, Singapore 487372, Singapore*

Zhengning Yang − *Division of Physics and Applied Physics, School of Physical and Mathematical Sciences, Nanyang Technological University, Singapore 637371, Singapore*

Weikang Gong − *College of Life Science and Chemistry, Faculty of Environmental and Life Sciences, Beijing University of Technology, Beijing 100124, China; Division of Mathematical Sciences, School of Physical and Mathematical Sciences, Nanyang Technological University, Singapore 637371, Singapore*

Complete contact information is available at: https://pubs.acs.org/10.1021/acs.nanolett.1c04705

Notes

The authors declare no competing financial interest.

ACKNOWLEDGMENTS

The authors thank D. L. Deng for helpful discussions. This work was supported by NSFC (11890703, 11975125) and Singapore MOE AcRF Tier 2 (MOE2019-T2-1-001). H.C. was also supported by China Scholarship Council. We acknowledge computational support from the Texas Advanced Computing Center.

REFERENCES

(1) Prelog, V. Chirality in chemistry. *Science* **1976**, *193*, 17−24.

(2) Cahn, R. S.; Ingold, C.; Prelog, V. Specification of molecular chirality. *Angewandte Chemie International Edition in English* **1966**, *5*, 385−415.

(3) Francotte, E.; Lindner, W.; Mannhold, R.; Kubinyi, H.; Folkers, G. *Chirality in drug research*; Wiley-VCH: Weinheim, 2006.

(4) Ma, L.; Abney, C.; Lin, W. Enantioselective catalysis with homochiral metal-organic frameworks. *Chem. Soc. Rev.* **2009**, *38*, 1248−1256.

(5) Reddy, I. K.; Mehvar, R. *Chirality in drug design and development*; CRC Press, 2004.

(6) Göhler, B.; Hamelbeck, V.; Markus, T.; Kettner, M.; Hanne, G.; Vager, Z.; Naaman, R.; Zacharias, H. Spin selectivity in electron transmission through self-assembled monolayers of double-stranded DNA. *Science* **2011**, *331*, 894−897.

(7) Guo, A.-M.; Sun, Q.-f. Spin-selective transport of electrons in DNA double helix. *Physical review letters* **2012**, *108*, 218102.

(8) Liu, Y.; Xiao, J.; Koo, J.; Yan, B. Chirality-driven topological electronic structure of DNA-like materials. *Nature materials* **2021**, *20*, 638−644.

(9) Zhang, L.; Niu, Q. Chiral phonons at high-symmetry points in monolayer hexagonal lattices. *Physical review letters* **2015**, *115*, 115502.

(10) Zhu, H.; Yi, J.; Li, M.-Y.; Xiao, J.; Zhang, L.; Yang, C.-W.; Kaindl, R. A.; Li, L.-J.; Wang, Y.; Zhang, X. Observation of chiral phonons. *Science* **2018**, *359*, 579−582.

(11) Chen, X.; Lu, X.; Dubey, S.; Yao, Q.; Liu, S.; Wang, X.; Xiong, Q.; Zhang, L.; Srivastava, A. Entanglement of single-photons and chiral phonons in atomically thin WSe 2. *Nat. Phys.* **2019**, *15*, 221−227.

(12) Li, Z.; Wang, T.; Jin, C.; Lu, Z.; Lian, Z.; Meng, Y.; Blei, M.; Gao, M.; Taniguchi, T.; Watanabe, K.; et al. Momentum-dark intervalley exciton in monolayer tungsten diselenide brightened via chiral phonon. *ACS Nano* **2019**, *13*, 14107−14113.

(13) He, M.; Rivera, P.; Van Tuan, D.; Wilson, N. P.; Yang, M.; Taniguchi, T.; Watanabe, K.; Yan, J.; Mandrus, D. G.; Yu, H.; et al. Valley phonons and exciton complexes in a monolayer semiconductor. *Nat. Commun.* **2020**, *11*, 1−7.

(14) Chen, H.; Wu, W.; Zhu, J.; Yang, S. A.; Zhang, L. Propagating Chiral Phonons in Three-Dimensional Materials. *Nano Lett.* **2021**, *21*, 3060−3065.

(15) Pandey, T.; Polanco, C. A.; Cooper, V. R.; Parker, D. S.; Lindsay, L. Symmetry-driven phonon chirality and transport in one-dimensional and bulk B a 3 N-derived materials. *Phys. Rev. B* **2018**, *98*, 241405.

(16) Grissonnanche, G.; Thériault, S.; Gourgout, A.; Boulanger, M.-E.; Lefrançois, E.; Ataei, A.; Laliberté, F.; Dion, M.; Zhou, J.-S.; Pyon, S.; et al. Chiral phonons in the pseudogap phase of cuprates. *Nat. Phys.* **2020**, *16*, 1108−1111.

(17) Park, S.; Yang, B.-J. Phonon angular momentum Hall effect. *Nano Lett.* **2020**, *20*, 7694−7699.

(18) Hamada, M.; Minamitani, E.; Hirayama, M.; Murakami, S. Phonon angular momentum induced by the temperature gradient. *Physical review letters* **2018**, *121*, 175301.

(19) Juraschek, D. M.; Spaldin, N. A. Orbital magnetic moments of phonons. *Physical Review Materials* **2019**, *3*, 064405.

(20) Cheng, B.; Schumann, T.; Wang, Y.; Zhang, X.; Barbalas, D.; Stemmer, S.; Armitage, N. P. A large effective phonon magnetic moment in a Dirac semimetal. *Nano Lett.* **2020**, *20*, 5991−5996.

(21) Romao, C. P. Anomalous thermal expansion and chiral phonons in BiB 3 O 6. *Phys. Rev. B* **2019**, *100*, 060302.

(22) Deal, B. E.; Helms, C. R. *The physics and chemistry of SiO_2 and the Si-SiO_2 interface*; Springer Science & Business Media, 2013.

(23) Glinnemann, J.; King, H., Jr; Schulz, H.; Hahn, T.; La Placa, S.; Dacol, F. Crystal structures of the low-temperature quartz-type phases of SiO2 and GeO2 at elevated pressure. *Zeitschrift für Kristallographie-Crystalline Materials* **1992**, *198*, 177−212.

(24) Antao, S. M.; Hassan, I.; Wang, J.; Lee, P. L.; Toby, B. H. State-of-the-art high-resolution powder X-ray diffraction (HRPXRD)

illustrated with Rietveld structure refinement of quartz, sodalite, tremolite, and meionite. *Canadian Mineralogist* **2008**, *46*, 1501−1509.
(25) Zhang, L.; Niu, Q. Angular momentum of phonons and the Einstein-de Haas effect. *Phys. Rev. Lett.* **2014**, *112*, 085503.
(26) Frenkel, V. Y. On the history of the Einstein-de Haas effect. *Soviet Physics Uspekhi* **1979**, *22*, 580.

https://doi.org/10.1021/acs.nanolett.1c04705
Nano Lett. 2022, 22, 1688−1693